Proceeding of the 7th International Symposium on Artificial Intelligence, Robotics and Automation in Space: i-SAIRAS 2003, NARA, Japan, May 19-23, 2003

The operation of flexible massive payload considering vibration suppression

Kazuya Konoue and Saburo Matunaga
Tokyo Institute of Technology
2-12-1 Oookayama, Meguro-ku, Tokyo, 152-8552, Japan
konoue@lss.mes.titech.ac.jp

Keywords Space Robotics, Contact/Push Motion Vibration Suppression, Input Shaping

Abstract

It is expected that autonomous space robots conduct many on-orbit servicings, for example the construction and maintenance of large space structures as well as the capture and recovery of damaged satellites. It is necessary to research on floating massive payload operation using robotic manipulators through both analytical and experimental approaches. We have conducted the ground experiment simulated on-orbit servicing. This ground experiment system is very useful to study strategies and approaches to capture damaged satellites and operation of floating massive payload in space. Next, we conduct the numerical simulation on manipulation of the flexible payload considering vibration suppression and will propose the appropriate control method of the robotic arm mounted on a satellite. We explain the experimental and analytical results of operation such as capturing the damaged satellite and operating the floating massive payload.

1. Introduction

It is expected that autonomous space robots conduct many on-orbit servicings, for example the construction and maintenance of large space structures as well as the capture and recovery of damaged satellites. In order to realize these missions, robot manipulators mounted on a satellite can be useful. In Japan, the Engineering Test Satellite VII (ETS-VII) was launched in 1997, and had experimented the robot operation technology as well as the rendezvous and docking technology until the end of 1999, which are indispensable to realize services in orbit. But there still exists many technical issues when an unmanned spacecraft deals autonomously with the floating massive payload, for example, design of a grasping mechanism and control methods to approach and grip the target, and to reduce the relative motion between the target and chaser and so on. Thus, it is necessary to research on floating massive payload operation using robotic manipulators through both analytical and experimental approaches. We have conducted the ground experiment simulated on-orbit servicing. This ground experiment system is very useful to study strategies and approaches to capture damaged satellites and operation of floating massive payload in space.

There are many problems, especially in berthing operation of a flexible payload. During the berthing operation of a flexible payload, the effect of the vibration of the robotic arm mounted on a satellite is not negligible. Moreover, there is a possibility of resonance between the arm vibration and the mounted flexible structure. In this study, we discuss the control of the operation of flexible massive payload considering vibration suppression. The vibration of the robotic arm mounted on a satellite in the berthing manipulation of flexible payload is characterized as follows. 1) The coupling between the arm and the satellite attitude vibration, 2) the transition of the natural frequency according to its posture changes with the inertial parameter variation, 3) the vibration of the flexible payload itself. Numerical simulations for the berthing manipulation are conducted considering the flexibility of the payload, and we understand the dynamics of the space robotic arm berthing operation.

Therefore we verify possibility of realization and operation sequence.

In this paper, we explain the results of ground experiment and numerical simulation on manipulation of the flexible payload and will propose the appropriate control method of the robotic arm mounted on a satellite.

2. Ground Experimental System

Figure 1 shows the tele-operation ground experiment system[1]. This system consists of the following subsystems: the simulated ground station system, simulated robot (chaser) satellite system and simulated target system.

The simulated robot satellite system consists of robot manipulator subsystem, mounted computer subsystem and vision system. The robot manipulator subsystem consists of a dual-manipulator, end-effectors and

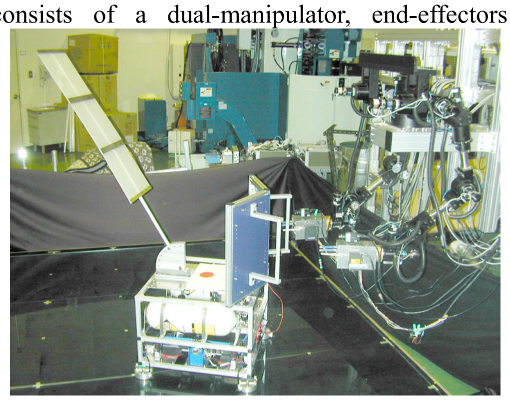

(a) Target Satellite Model and Dual-Manipulator

(b) Tele-operation System

Fig.1 Overview of the Ground Experiment

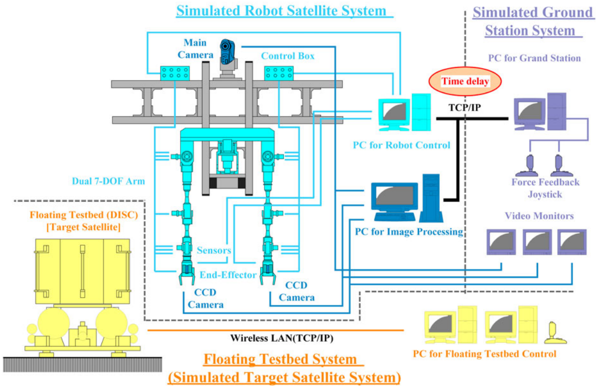

Fig.2 Scehmatic of the Ground Experiment

actuator control boxes. The dual-manipulators simulate space manipulators mounted on a chaser satellite, and are fixed on the ground, and each arm is a 7-DOF human arm type manipulator. The dual-manipulator can be operated with joysticks as shown in Figure 2. The end-effector has a grip mechanism, CCD camera, laser displacement sensor and six-axis force/torque sensor. The grip mechanism is designed to grip handrails and a solar paddle beam of the simulated target satellite. The target system, whose mass is about 50kg, is a floating testbed with handrails and simulated solar paddle[2]. The flat floor is covered with a plate grass and has 3m x 5m in area. The feature of this ground experiment system is combining the robot manipulator system and the simulated target satellite, which moves freely in the two-dimensional space.

This system uses the LAN (Local Area Network) for the communications between the simulated ground station and the robot satellite, and therefore can introduce the random time lag in communication, which is one of the important problems in tele-operating the satellites. As shown as Figure 3, the time delay is controlled by the time delay server, therefore we can vary communication time delay in

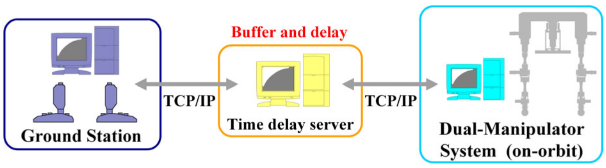

Fig.3 Communication Block diagram

this system. The time delay sever receives command or telemetry, and buffers them. After the delayed time, they are sent to on-orbit system or ground station.

3. Kinematics and Control

3.1 Kinematical Analysis of Dual-Manipulator

Dual-Manipulator and Coordinate Systems

Figure 4 shows the coordinate systems used in kinematics analysis. The coordinate system fixed at the main satellite $\{\boldsymbol{b}_0\}$ is identical to the absolute coordinate system $\{\boldsymbol{i}\}$ in this case, and $\{\boldsymbol{b}_{ir}\}$ and $\{\boldsymbol{b}_{il}\}$ (i=1,…,7) are i-th joint fixed coordinate systems of the right and the left manipulator, respectively. The subscripts r and l stand for parameters of the right and left manipulator, respectively.

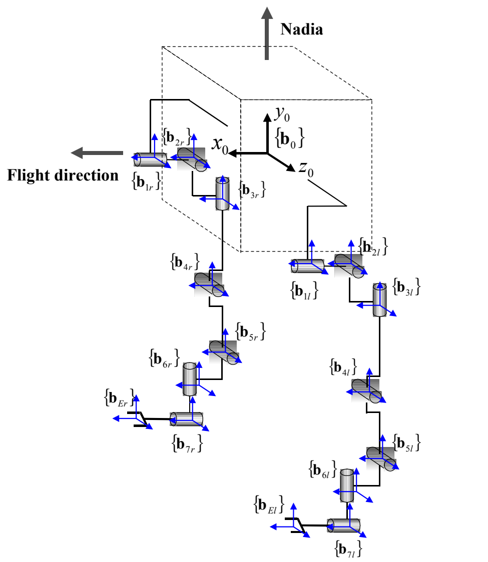

Fig.4 Coordinate systems on dual-manipulator

Direct Kinematics

The end-effector position vectors p_{Er} and $\mathrm{p}_{El} \in \Re^3$ in $\{\boldsymbol{b}_0\}$ are obtained from the joint angles θ_{ir} and θ_{il} by the following relationships:

$$\begin{aligned}\mathrm{p}_{Es} &= \bar{\mathrm{l}}_{0s} + \bar{\mathrm{R}}^2_{1s}\left(\bar{\mathrm{l}}_{1s} + \bar{\mathrm{R}}^1_{2s}\left(\bar{\mathrm{l}}_{2s} + \bar{\mathrm{R}}^3_{3s}\left(\bar{\mathrm{l}}_{3s} + \bar{\mathrm{R}}^1_{4s}\left(\bar{\mathrm{l}}_{4s} + \bar{\mathrm{R}}^1_{5s}\left(\bar{\mathrm{l}}_{5s} + \bar{\mathrm{R}}^3_{6s}\left(\bar{\mathrm{l}}_{6s} + \bar{\mathrm{R}}^2_{7s}\bar{\mathrm{l}}_{7s}\right)\right)\right)\right)\right)\right) \\ &= \mathrm{l}_{0s} + \mathrm{l}_{1s} + \mathrm{l}_{2s} + \mathrm{l}_{3s} + \mathrm{l}_{4s} + \mathrm{l}_{5s} + \mathrm{l}_{6s} + \mathrm{l}_{7s}\end{aligned} \qquad (\mathrm{s} = \mathrm{r, l}), \ (3.1.1)$$

where $\bar{\mathrm{R}}^k_{is}$ (k =1,2,3, i =1,…,7, s = r, l) $\in \Re^{3\times3}$ are rotation matrices, which are

$$\bar{\mathrm{R}}^1_{\mathrm{is}} = \begin{bmatrix} 1 & 0 & 0 \\ 0 & \cos\theta_{\mathrm{is}} & -\sin\theta_{\mathrm{is}} \\ 0 & \sin\theta_{\mathrm{is}} & \cos\theta_{\mathrm{is}} \end{bmatrix}$$

$$\bar{\mathrm{R}}^2_{is} = \begin{bmatrix} \cos\theta_{is} & 0 & \sin\theta_{is} \\ 0 & 1 & 0 \\ -\sin\theta_{is} & 0 & \cos\theta_{is} \end{bmatrix}$$

$$\bar{\mathrm{R}}^3_{is} = \begin{bmatrix} \cos\theta_{is} & -\sin\theta_{is} & 0 \\ \sin\theta_{is} & \cos\theta_{is} & 0 \\ 0 & 0 & 1 \end{bmatrix} \qquad (3.1.2)$$

and $\bar{\mathrm{l}}_{is}$ and $\mathrm{l}_{is} \in \Re^3$ (i=0,…,7) are link vectors in $\{\boldsymbol{b}_{is}\}$ and $\{\boldsymbol{b}_0\}$, respectively, which represent the relative position between the origins of $\{\boldsymbol{b}_{is}\}$ and $\{\boldsymbol{b}_{(i+1)s}\}$.

The end-effector attitudes R_{7r} and R_{7l} with respect to $\{\boldsymbol{b}_0\}$ are obtained by the following relations:

$$\mathrm{R}_{7s} = \bar{\mathrm{R}}^2_{1s}\bar{\mathrm{R}}^1_{2s}\bar{\mathrm{R}}^3_{3s}\bar{\mathrm{R}}^1_{4s}\bar{\mathrm{R}}^1_{5s}\bar{\mathrm{R}}^3_{6s}\bar{\mathrm{R}}^2_{7s} \qquad (\mathrm{s} = \mathrm{r, l}), \ (3.1.3)$$

These are transformed to the Roll-Pitch-Yaw angles $\mathrm{e}_{Es} = [\alpha_{Es} \quad \beta_{Es} \quad \gamma_{Es}]^T$ as follows,

$$\beta_{Es} = \mathrm{atan}\,2\left\{-\mathrm{R}_{7s}(1,3), \sqrt{\mathrm{R}_{7s}(3,3)^2 + \mathrm{R}_{7s}(2,3)^2}\right\}$$
$$(-\pi/2 \le \beta_{Es} \le \pi/2) \ (s = r, l), \qquad (3.1.4a)$$

$$\gamma_{Es} = \ \mathrm{atan}\,2\left\{\mathrm{R}_{7s}(2,3)/\cos\beta_s,\ \mathrm{R}_{7s}(3,3)/\cos\beta\right\}$$
$$(-\pi < \gamma_{Es} \le \pi) \qquad (s = r, l), \qquad (3.1.4b)$$

$$\alpha_{Es} = \ \mathrm{atan}\,2\left\{\mathrm{R}_{7s}(1,2)/\cos\beta_s,\ \mathrm{R}_{7s}(1,1)/\cos\beta\right\}$$
$$(-\pi < \alpha_{Es} \le \pi) \qquad (s = r, l), \qquad (3.1.4c)$$

where $\mathrm{R}_{7s}(i, j)$ is an i-j component of R_{7s}. Note that $\beta_{Es} = \pm\,\pi/2$ are singular.

Inverse Kinematics

The velocity equations are obtained from eqs.(3.1.1, 3) as follows,

$$\dot{\mathrm{r}}_s = \mathrm{J}_s(\theta_s)\dot{\theta}_s \quad (\mathrm{s} = \mathrm{r, l}), \qquad (3.1.5)$$

where $\mathrm{r}_s^T = \left[\mathrm{p}_{Es}^T \quad \mathrm{e}_{Es}^T\right] \in \Re^6$, $\theta_s^T = \left[\theta_{1s} \quad \cdots \quad \theta_{7s}\right] \in \Re^7$. J_s is a Jacobian matrix expressed as

$$\mathrm{J}_s(\theta_s) = \begin{bmatrix} \tilde{\mathrm{s}}_{1s}(\mathrm{p}_{Es} - \mathrm{p}_{1s}) & \tilde{\mathrm{s}}_{2s}(\mathrm{p}_{Es} - \mathrm{p}_{2s}) & \cdots & \tilde{\mathrm{s}}_{7s}(\mathrm{p}_{Es} - \mathrm{p}_{7s}) \\ \mathrm{s}_{1s} & \mathrm{s}_{2s} & \cdots & \mathrm{s}_{7s} \end{bmatrix}$$

$$\in \Re^{6\times7} \quad (\mathrm{s} = \mathrm{r, l}), \tag{3.1.6}$$

where s_{is} and p_{is} (i=1,…,7) $\in \Re^3$ are rotation axis matrices and i-th joint position matrices in $\{\boldsymbol{b}_0\}$, respectively. The tilde operator (~) is the operator concerned with vector cross product.

The Jacobian matrix is not a square matrix because of the redundancy of the dual-manipulator, then we can use the pseudo-inverse matrix to compute inverse kinematics from eq.(3.1.5). In this study, the task of the dual-manipulator is ground experiments for services in orbit such as damaged satellite capturing and berthing mission. When the following subtasks are carried out during the main task, the redundancy of the dual-manipulator is effectively used.

1. collision avoidance of the manipulator from the main satellite, the attached structures and the target object,
2. avoidance from the mechanical limitation with respect to the joint rotations,
3. avoidance of the kinematic singularities of the manipulators,
4. realization of the coordinated control to minimize the attitude disturbance of the main satellite.

Because we use the existing dual-manipulator, there are difficulties in use of the redundancy. As far as our experiments are concerned, the subtask 2 and 3 are effective. Furthermore, we have found that the subtask 2 is the most important in our manipulator system. We then apply the generalized inverse matrix with weighting matrix with respect to joint rotation limits given as

$$\mathrm{J}_s^+ = \mathrm{W}_s^{-1}\mathrm{J}_s^T\left(\mathrm{J}_s\mathrm{W}_s^{-1}\mathrm{J}^T\right)^{-1} \quad (s = r, l), \tag{3.1.7}$$

where $\mathrm{W}_s \in \Re^{7\times7}$ is a weighting matrix in the form of a diagonal matrix defined as

$$\mathrm{W}_s = \mathrm{diag}\left\{\frac{1}{(\theta_{1s,\max} - \theta_{1s})^2} + \frac{1}{(\theta_{1s} - \theta_{1s,\min})^2} \quad \cdots \quad \frac{1}{(\theta_{7s,\max} - \theta_{7s})^2} + \frac{1}{(\theta_{7s} - \theta_{7s,\min})^2}\right\} \tag{3.1.8}$$

$\theta_{is,\max}$ and $\theta_{is,\min}$ (i=1,…,7, s=r,l) are the maximum and minimum angles of each joint, respectively.

3.2 Kinematical Control of Dual-Manipulator

In this study, we use a Resolved Motion Rate Control(RMRC) for control of dual-manipulator system. An RMRC mode is to control manipulators by a control command formed from the set of position (x, y, z) and attitudes (roll, pitch, yaw) data of the end-effector.

This mode is normally applied to operate manipulators. This mode has a problem that an input rotation speed overflows when the configuration of the manipulator is singular. Our system stops and/or gives a warning to the operator when the configuration is getting singular. We use the measure of manipulability

$$\omega = \sqrt{\det \mathrm{JJ}^T} \tag{3.2.1}$$

defined by Yoshikawa[3] as the index of singularity.

4. Contact/Push Motion

The concept of the contact/push-based motion control method is proposed in 1999[4]. The operation sequences for the chaser to make contact are described as follows:

Phase 1. Observation and planning.

Phase 2. Approach and contact.

Phase 3. Separation and preparation.

In Phase 1, the chaser is required to observe the target's motion using an onboard visual sensor, and plan the contact operation. In Phase 2, the flexible end-effector, which can be attached to the arm tip, softly touches the target surface so as to damp the target's angular momentum. The chaser makes the end-effector approach the selected contact area on the target without following its rotational motion. The approach operation is conducted using the relative motion information between the end-effector and the target. After contact, forces such as friction between the end-effector and target's surface caused by sliding and/or the pushing force opposing the rotational motion, are indirectly controlled by the deflection of the flexible end-effector. The arm is usually controlled kinematically during the approach and contact sequence, so this method is clearly different from the impedance control of the robotic arm. Thus, the angular momentum can be reduced without changing the mode of the arm. Moreover, because the flexible end-effector is also available as an impulsive damper, a rigid body collision between the chaser and the target in capture sequence can be avoided. In Phase 3, the chase is required to compensate for its attitude and the distance from the target by actuators such as reaction wheels and gas jet thrusters. These sequences are repeated until the magnitude of the target's angular momentum decreases sufficiently. In this paper, the experimental results of Phase 2 motion are described.

4. Ground Experiment

4.1 Experiment of Capturing and Berthing Target

The right-arm is directly used for capturing the handrail of the satellite and berthing the satellite body, and visual information is obtained with the main camera installed on the dual-manipulator system body and two cameras equipped at each end-effectors. In this experiment, the left-arm is used for providing a movable vision which is a very important and vital tool in closely proxy tasks such as a capture operation. The following experiments are conducted in order to check the usefulness of the movable view by the left-arm (left hand-eye camera). From the figures, the operator can judge the right end-effector situation, inspect the neighborhood of the handrail, and understand the grasping conditions. During the operation, the operators reported that the tasks are more easily accomplished even just before grasping. Figure 5 shows the data of (a) end-effector trajectory, and (b) force/torque sensor output, and (c) distance between end-effector and handrail, and indicates the open/close states of the end-effector.

Next, we have introduced random time lag, 10 seconds delay, to communication between the simulated ground station and the robot satellite. During

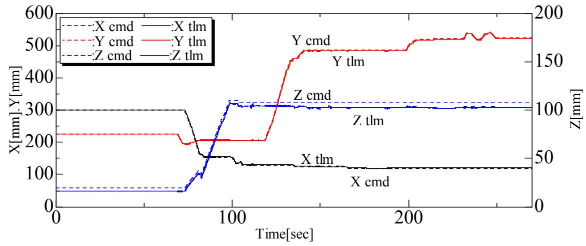

(a) End-effector trajectory

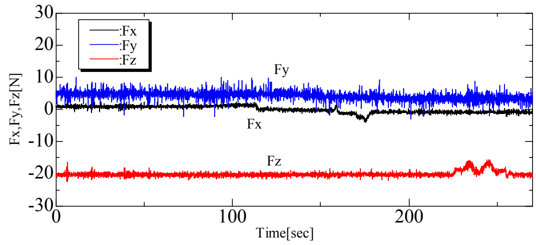

(b) Force/torque sensor output

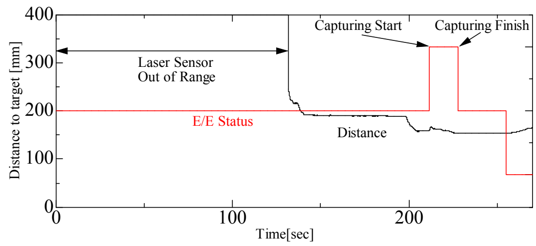

(c) Distance between end-effector and handrail

Fig.5 Results of satellite capturing experiment

the operation, the operators reported that it is hard to understand the situation nearby the end-effector, and worried about manipulating, therefore the tasks are not easily accomplished. Moreover, because of the delay of the information on the distance, the operator has made the end-effector nearly collide with the handrail. Therefore, it is necessary to implement the autonomous mode for avoiding collision, introducing the predictive display of the dual- manipulator with CG.

4.2 Experiment of Contacting/Pushing Target

In order to realize the capture of more general targets, it may be difficult for the space-robotic arm to grip them directly. In view of this, it is necessary to seek out other ways to subdue the relatively large rotational motions of the target without direct gripping, and assist the capture operations using robotic arm.

Therefore, the method, called contact/push-based control, in which a robotic arm uses a flexible end-effector to contact the target, has been proposed. In this experiment, we will investigate the usefulness for this method based on contact/push control for the rotational target without following its motion. The chaser makes the flexible end-effector approach and contact to the target surface, the angular momentum of the target is decreased using the contact forces, such as pushing force dragged to the rotation motion and/or friction force caused by sliding the surface. As shown in Figure 6, a cushion-type damper is attached to the end-effector of the arm, and the arm softly pushes the damper on a selected point on the target. The initial angular velocity of the target is 12 deg/s. The direction of contact force is opposition to the target's rotational motion, and the end-effector waits for the target to be contacted.

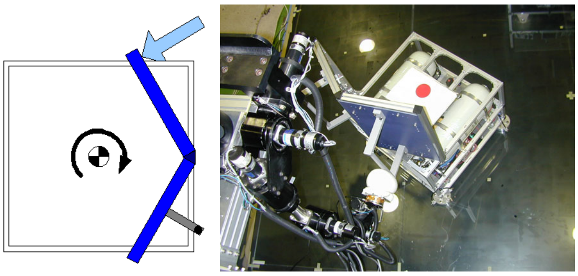

Fig.6 Contact point and contact/push motion

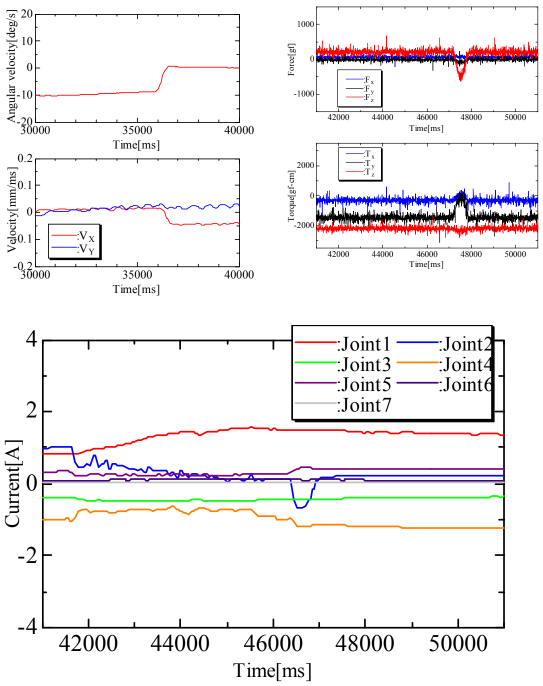

Fig. 7 Experimental results of contact/push-based

Figure 7 shows angular velocity and velocity of the target, force/torque sensor output, and currents through the actuator on each joint of dual-manipulator. Figure 7 shows that the reduction of the target's angular velocity is achieved, and currents on each joint of manipulator are low. Thus from this experimental result, the repeated contact/push based control can decrease the target angular momentum sufficiently small and the usefulness of this method is shown.

5. The robotic operation considering vibration suppression

There are many problems, especially in berthing operation of a flexible payload. During the berthing operation of a flexible payload, the effect of the vibration of the robotic arm mounted on a satellite is not negligible. Moreover, there is a possibility of resonance between the arm vibration and the mounted flexible structure. In this study, we discuss the control of the operation of flexible massive payload considering vibration suppression. We apply Input Shaping in order to suppress the vibration. Input Shaping is a feedforward control technique for reducing vibration. The method works by creating a command signal that cancels its own vibration. That is, vibration caused by the first part of the command signal is canceled by vibration caused by the second of the command[5]. We conduct numerical simulations for the berthing manipulation considering the flexibility of the payload. Figure 8 shows analytical model. The robotic arm is a 7-DOF human arm type manipulator and the payload has flexibility. First, we understand the dynamics of the space robotic arm berthing operation. Next, we apply Input Shaping to operation method of the robotic arm in order to suppress the vibration. Therefore we verify possibility of realization and operation sequence.

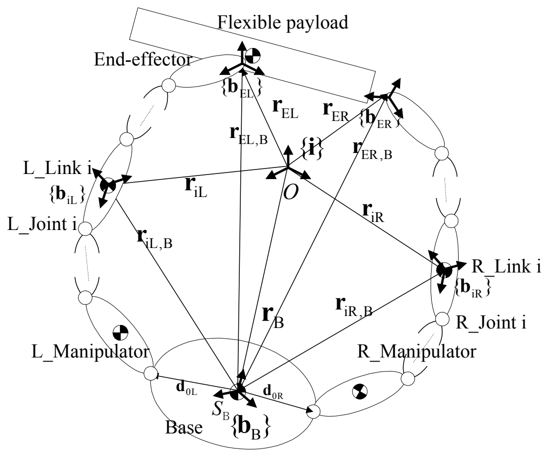

Fig.8 The analytical model

6. Conclusion

We explained the ground experiment system for fundamental study of operating methods of the target using the dual-manipulator. We examined the method of operating the target using camera images, which provides some hints for a feasible automatic capturing method. Next, we investigated the usefulness of contact/push-based control for the rotational target, which is the method to reduce the angular momentum of the target using a flexible end-effector, experimentally. Moreover, we discuss the control of the operation of flexible massive payload considering vibration suppression. We apply Input Shaping in order to suppress the vibration, and discuss the more effective strategy of the robotic operation of the flexible payload. The ground experimental system enables us to plan the efficient operating strategies and cooperative activities of the dual-manipulator in space.

Reference

[1] K. Konoue, N. Miyashita and S. Matunaga, "Experimental Study for Dual-Manipulator-Based Operation of Floating Massive Payload," International Symposium on Artificial Intelligence, Robotics and Automation in Space (i-SAIRAS), Montreal, Canada, June, 2001.

[2] H. Okada, S. Tsurumi and S. Matunaga, "Development and Functional Evaluation Experiments of Robot Satellite Cluster Simulator System," 23rd International Symposium on Space Technology and Science, Matsue, May, 2002.

[3] T. Yoshikawa, "Analysis and Control of Robot Manipulators with Redundancy," Robotics Research: The First Interntl Symp, (M. Brady and R. Paul ed.), MIT Press, Cambridge, MA. pp.735-747, 1984.

[4] S. Matunaga, T. Kanzawa and Y. Ohkami, “Rotational motion-damper for the capture of an uncontrolled floating satellite,” Control Engineering Practice, Vol.9, pp.199-205, 2001

[5] W. Singhose and W. Seering, "Analytic Methods for Slewing Undamped Flexible Structures with On-Off Actuators," AIAA Guidance, Navigation, and Control Conf. New Orleans, LA, 1997